Contribution from the Department of Chemistry,
University of Delaware, Newark, Delaware 19716

Thermal Decomposition of Energetic Materials. 34. Decarbonylation, Decarboxylation, and Coupling Reactions of Metal Propiolates, $M[O_2CC{\equiv}CH]$

C. E. Stoner, Jr., and T. B. Brill*

Received May 10, 1989

The thermal decomposition of metal propiolate salts, $M[O_2CC{\equiv}CH]_x{\cdot}y[HO_2CC{\equiv}CH]{\cdot}zH_2O$, where M = Na ($x = 1$, $y = 0$, $z = 0$), K ($x = 1$, $y = 0$, $z = 0$), Rb ($x = 1$, $y = 0.5$, $z = 0$), Co ($x = 2$, $y = 0$, $z = 3$), Ni ($x = 2$, $y = 0$, $z = 0$), and Zn ($x = 2$, $y = 0$, $z = 2$), is described for slow heating by TGA, DSC, and IR spectroscopy and for fast heating (80-300 °C/s) by FTIR/temperature profiling. The decomposition temperatures and ΔH_{dec} of the Na^+, K^+, and Rb^+ salts predict their tendency to thermalize by decarbonylation, decarboxylation, or coupling when in the unconfined state. Decarbonylation yields M_2CO_3, CO, C, and C_2H_2, while decarboxylation yields M_2CO_3, CO_2, C, and C_2H_2. Coupling leads to a solid product resembling an acetylenedicarboxylate salt. The CO/CO_2 and C_2H_2/CO_x gas product ratios for these salts support these descriptions. A lower decomposition temperature, lower lattice energy, and smaller ΔH of decomposition favors decarboxylation and coupled products (Rb^+), while the reverse favors decarbonylation (Na^+, K^+). Extensions of these notions to the Co^{2+}, Ni^{2+}, and Zn^{2+} salts indicate that the decomposition temperature reliably predicts their tendency to decarbonylate and form a carbonate (Ni^{2+}), or decarboxylate and form coupled products (Co^{2+}, Zn^{2+}). All six salts give evidence of coupling when slowly thermalized between two BaF_2 plates.

Introduction

Metal propiolate salts, $M[O_2CC{\equiv}CH]$, partially polymerize to poly(propiolate) salts when exposed to X- or γ-radiation for hours to weeks.[1-5] Moreover, Foxman[4] found that $M[O_2CC{\equiv}CH]_2{\cdot}4H_2O$, where M = Co and Ni, explode on heating. Our interest in understanding the ignition and explosion chemistry of metal complexes[6,7] attracted us to these salts. The possibility that an explosive, solid-state polymerization occurs was especially intriguing because a voluminous, fragile residue is rapidly produced upon thermal decomposition.[8]

The slow and rapid thermal decomposition of group IA (Na^+, K^+, Rb^+) and first-row transition-element (Co^{2+}, Ni^{2+}, Zn^{2+}) propiolate salts is described in this paper. Several of the compounds were found to exist with more than one stoichiometry and differed from those studied by Foxman et al.,[3-5,8] so we decided to gather all of the data necessary for this project on samples characterized in-house. The slow thermolysis was characterized by TGA, DSC, and transmission IR spectroscopy, while rapid thermolysis was studied by temperature profiling/FTIR spectroscopy.[9,10] Coupling-like reactions occurred in all of the salts when the sample was confined between BaF_2 plates and slowly heated. The Rb^+, Zn^{2+}, and Co^{2+} salts also give evidence of coupling reactions in the unconfined state. The term "coupling" is used here because it was not established whether these products are polymers. There is spectral evidence for coupling, but further work on this avenue was not the purpose of this project. Comments about the possible nature of poly(propiolate) salts formed by X- and γ-radiation have been given by Davidov et al.[1] and Foxman et al.[4,5]

The motivation to investigate the explosive nature was set aside early in the project because the vigorous off-gassing during thermolysis appeared to be more characteristic of gas generator materials than of explosives. This is probably because these propiolate salts are fuel-rich and so their thermal decomposition does not generate the concerted energy release and reaction rates characteristic of explosives. However, if mixed with an oxidant, these compounds are potentially quite energetic. This is because the C≡C bond has approximately 460 kJ/mol more energy than the C—C bond. A characterization of the thermal decomposition of energy-rich fuel salts fits our objective to understand the thermolysis of energetic metal complexes.[6,7] Detailed studies were conducted on the Na^+, K^+, and Rb^+ salts because their similarity enabled the decomposition patterns to be established. These patterns were then carried over to understand the results for a nonhomologous series of salts of divalent cations and to underpin the validity of the mechanisms.

Experimental Section

Compounds. Samples of several propiolate salts including Na^+, K^+, and Rb^+ were generously supplied by B. M. Foxman of Brandeis University. We characterized the samples in hand to be $Na[O_2CC{\equiv}CH]$, $K[O_2CC{\equiv}CH]$ and $Rb[O_2CC{\equiv}CH]{\cdot}0.5[HO_2CC{\equiv}CH]$ by elemental analysis (MicroAnalysis, Wilmington, DE), differential scanning calorimetry (DSC), thermogravimetric analysis (TGA), and IR spectroscopy. These salts are somewhat hygroscopic so they were carefully dried in a vacuum prior to use. For instance, the potassium salt was proven to be able to exist as $K[O_2CC{\equiv}CH]{\cdot}H_2O$, but the H_2O could be removed by drying. Purple $Co[O_2CC{\equiv}CH]_2{\cdot}3H_2O$, light brown $Ni[O_2CC{\equiv}CH]_2$, and pale orange $Zn[O_2CC{\equiv}CH]_2{\cdot}2H_2O$ were prepared by adding a 1:2 molar ratio of the metal oxide to colorless propiolic acid in H_2O and stirring for 40 min. The solution was filtered through Celite and placed in a covered beaker to evaporate until crystals formed. The crystals were removed and dried at 10^{-2} Torr for 12 h. The samples were stored in a vacuum desiccator. Anal. Calcd for $C_6H_8O_7Co$: C, 28.70; H, 3.18. Found: C, 28.73; H, 2.66. Calcd for $C_6H_2O_4Ni$: C, 36.60; H, 1.01. Found: C, 37.23; H, 1.48. Calcd for $C_6H_6O_6Zn$: C, 30.08; H, 2.17. Found: C, 31.40; H, 2.18. The H_2O content of several of these salts differs from those characterized by Foxman et al.[5] probably because our samples were dried at low pressure. Studies were performed on an internally consistent set of samples for this paper. Red $Co[O_2CC{\equiv}CH]_2{\cdot}4H_2O$, was supplied by B. M. Foxman. Potassium acetylenedicarboxylate was prepared by neutralization of KHC_4O_4 (Aldrich) with KOH.

IR Spectra. Spectra of the solid phases during slow thermal decomposition were obtained by using a transmission spectroscopy cell equipped for slow, controlled heating.[11] Usually BaF_2 plates were used to support a thin film of the sample; however, NaCl was also occassionally used. BaF_2 proved to be the least prone to ion exchange of the various IR-transparent windows tried. In most cases, the sample was burnished onto the plates, but in several instances where the effect of the solvent was known, the sample was dissolved and placed on the plate by evaporation. The IR spectra were recorded by using a Nicolet 60SX FTIR spectrometer at 2-cm^{-1} resolution with 36 scans added in each file.

Rapid thermal decomposition studies were performed with the temperature-profiling/FTIR technique developed in our laboratory.[9,10] Typically, 1 mg of sample was thinly spread on the nichrome ribbon filament in the cell. The sample was heated at a chosen rate between 80 and 300 °C/s while the gases 3 mm above the surface were monitored simultaneously in real time by FTIR spectroscopy (Nicolet 60SX, 10 scans/s, 2 spectra/file, 4-cm^{-1} resolution), while the temperature of the

(1) Davidov, B. E.; Krenstel, B. A.; Kchutareva, G. V. *J. Polym. Sci.* **1967**, *C16*, 1365.
(2) Neilsen, G. W.; Symons, M. C. R. *J. Chem. Soc., Perkin Trans.* **1973**, *2*, 1405.
(3) Foxman, B. M.; Jaufmann, J. D. *J. Polym. Sci., Polym. Symp.* **1983**, *70*, 31.
(4) Foxman, B. M.; Jaufmann, J. D. *Mol. Cryst. Liq. Cryst.* **1984**, *106*, 187.
(5) Booth, C. A.; Foxman, B. M.; Jaufmann, J. D. *ACS Symp. Ser.* **1987**, *No. 337*, 95.
(6) Palopoli, S. F.; Brill, T. B. *Combust. Flame* **1988**, *72*, 153.
(7) Palopoli, S. F.; Brill, T. B. *Inorg. Chem.* **1988**, *27*, 2971.
(8) Foxman, B. M. Personal communication, 1988.
(9) Cronin, J. T.; Brill, T. B. *Appl. Spectrosc.* **1987**, *41*, 1147.
(10) Cronin, J. T.; Brill, T. B. *Appl. Spectrosc.* **1989**, *43*, 650.
(11) Karpowicz, R. J.; Brill, T. B. *Appl. Spectrosc.* **1983**, *37*, 79.
(12) Oyumi, Y.; Brill, T. B. *Combust. Flame* **1985**, *62*, 213.

0020-1669/89/1328-4500$01.50/0

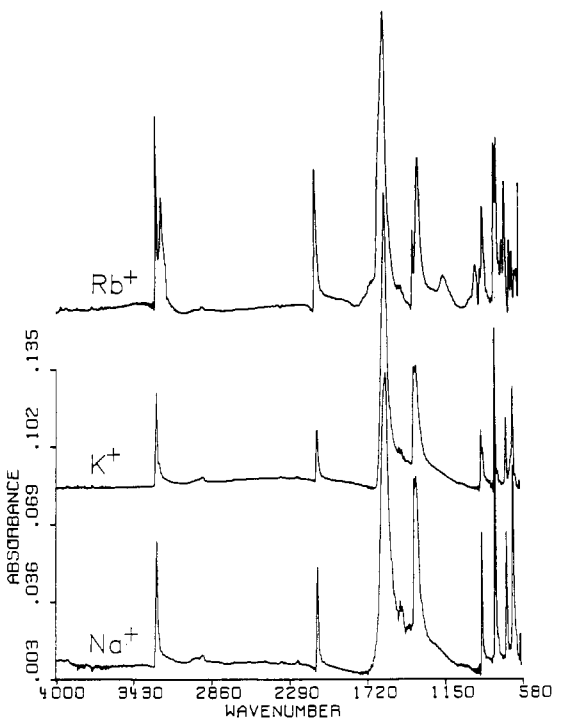

Figure 1. Transmission IR spectra of neat $Na[O_2CC{\equiv}CH]$, $K[O_2CC{\equiv}CH]$, and $Rb[O_2CC{\equiv}CH]{\cdot}0.5[HO_2CC{\equiv}CH]$.

condensed phase was monitored in real time by a type E thermocouple spot-welded to the underside of the filament. The output of the thermocouple was monitored with an IBM PC through a Metrabyte DAS-16 AD converter. The static pressure of Ar in the cell was set as desired in the 1–1000 psi range. A reference thermal trace was recorded with no sample on the filament, and then the temperature trace and spectral run were made simultaneously with the sample present. The gases evolved into the cool Ar atmosphere where they were quenched, and their IR spectra were recorded in the rapid-scan mode. Thus, a near-real-time measurement of the evolved gases next to the surface of the sample can be obtained simultaneously with the temperature changes in the condensed phase that produce these gases. The relative percent concentration of each gas was obtained by using their absolute intensity values.[12]

TGA and DSC. Thermal analysis measurements were made on a Du Pont Instruments Model 2000 analyzer equipped with a standard Model 910 DSC and Model 951 TGA head. The heating rate for both the DSC and TGA measurements was 5 °C/min. A static N_2 atmosphere was used unless otherwise noted. Typically 1–2 mg of sample was used for the TGA and 1–4 mg was used for the DSC measurements.

Slow Thermal Decomposition of $M[O_2CC{\equiv}CH]$ ($M = Na^+$, K^+, Rb^+)

The TGA, DSC, and IR spectra of slowly heated samples are described in this section. The findings are corroborated and detailed further by the rapid-heating, gas evolution studies described in the next section. Figure 1 shows the transmission IR spectrum of a thin film of a dried sample of each salt on an NaCl plate. As expected, the Na^+ and K^+ salts are very similar, while the Rb^+ salt reflects the fact that it is an acid solvate. Several of the modes are doubled in the Rb^+ salt. If this acid is removed by heating, the spectrum of the residue closely resembles those of the Na^+ and K^+ salts. However, the decomposition of the Rb^+ salt is quite different from the equivalent Na^+ and K^+ salts.

$Na[O_2CC{\equiv}CH]$. By DSC, a dried sample of sodium propiolate displays a small exotherm at 175 °C (5 J/g) followed by a large exotherm centered at about 203 °C (1250 ± 100 J/g). A voluminous, fragile, black material is blown from the sample at the second exotherm. Because of this, thermogravimetric analysis is difficult. Considerable effort was expended to obtain reasonably reliable data. No weight loss occurs during the first exotherm. However, about 25% of the weight was lost and the sample turned black at the second exotherm when the analysis was performed in an N_2 atmosphere. If the residue is then cooled to 25 °C under an N_2 blanket, it is found to be Na_2CO_3 based on comparison with an authentic sample. No C≡C, C=C, or C—H modes were

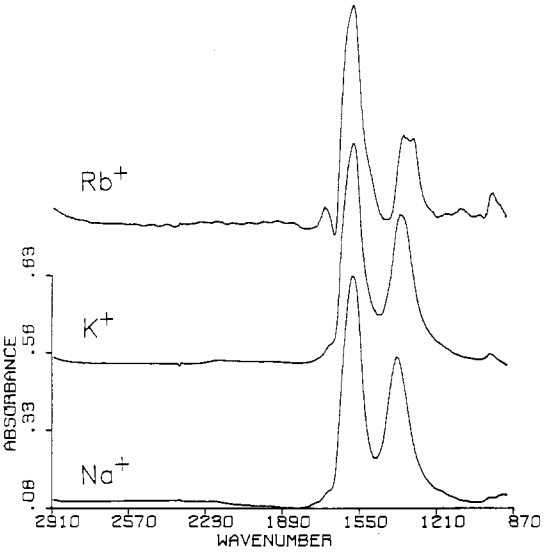

Figure 2. IR spectra of the products of slow thermal decomposition at about 210 °C of the propiolate salts of Na^+, K^+, and Rb^+ between BaF_2 plates showing the presence of a carboxylate residue without C≡C or C=C modes.

detected. A small amount of $Na_2C_2O_4$ is also present (<8%). The color of the sample and the IR spectrum suggest that the dominant decomposition process is described by the decarbonylation reaction 1. The approximate weight loss measured in the TGA is rec-

$$2Na[O_2CC{\equiv}CH] \xrightarrow{\Delta} Na_2CO_3 + CO + C_2H_2 + 2C \quad (1)$$

oncilable with reaction 1. The carbon generated will be largely amorphous under these experimental conditions and is responsible for the black color of the sample. Of course, it does not produce mid-IR modes. Confirmation and further details on the gas products will be given in the Fast Thermal Decomposition section (vide infra). The gases produce rapid intumescence of the sample, but the solid residue knits together as a voluminous, extremely fragile, spongelike material. Upon further heating of this material to 600 °C, the amorphous carbon reacts, probably with trace O_2 in the cell, to lighten the color of the residue. The residue in the TGA at 600 °C is 57% of the original weight, which corresponds closely to that of pure Na_2CO_3. In fact, if the thermolysis process is performed in air, where excess O_2 is always available, the sample remains white throughout and the only solid residue is Na_2CO_3. Thus, thermolysis of $Na[O_2CC{\equiv}CH]$ in the unconfined state with an oxidizing or an inert atmosphere gives no evidence of coupling reactions. Mainly decarbonylation occurs, leading to the products of reaction 1.

The slow thermal decomposition of a thin film of $Na[O_2CC{\equiv}CH]$ supported between two BaF_2 plates yields a different result. The gas products are unable to escape quickly and appear to mediate the reaction. The changes occurring in the sample were followed by IR spectroscopy at 5 °C intervals with a heating rate of 5 °C/min. There is only normal line broadening in the mid-IR modes up to 194 °C where DSC and TGA measurements showed that decomposition begins. The small exotherm at 175 °C in the DSC does not produce any change in the IR spectrum and, thus, is ruled out as a polymerization step. At about 194 °C, the C≡C and C—H modes begin to diminish in intensity and disappear entirely by 205 °C. Broad absorbances at 1577 and 1380 cm^{-1} grow in their place. The IR spectrum of the brown residue is shown in Figure 2. Probably because of the brown color, no Raman spectra could be obtained. Attempts were made to identify the residue by comparing its spectrum to those of authentic samples of likely products. The product is not a formate because the $-CO_2^-$ modes do not match an authentic sample and no C–H mode is present.[13,14] Further insight into the composition of the

(13) Donaldson, J. D.; Knifton, J. F.; Ross, S. D. *Spectrochim. Acta* **1964**, *20*, 847.

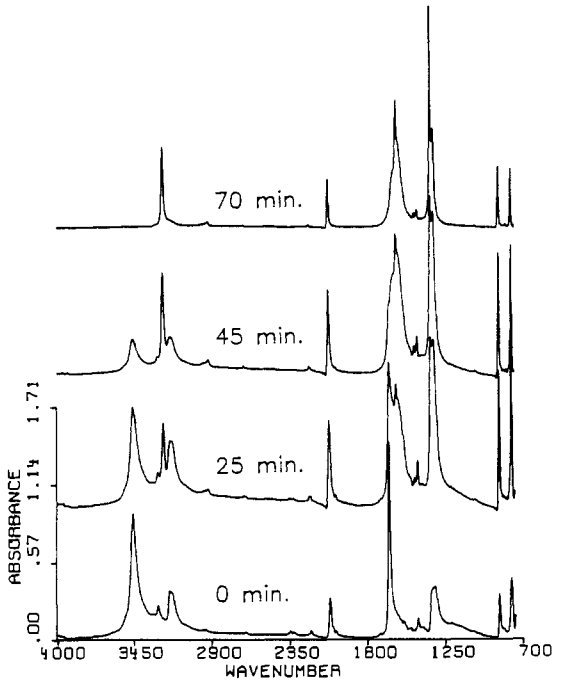

Figure 3. IR spectra of $K[O_2CC{\equiv}CH]$ on a BaF_2 plate immediately after evaporation of an $MeOH/H_2O$ solution (time = 0 min). The sample is $K[O_2CC{\equiv}CH]{\cdot}H_2O$. Note that H_2O gradually leaves the sample and the carboxylate group returns to the coordination sphere, giving $K[O_2CC{\equiv}CH]$ after 70 min.

residue was gained in the following study of potassium propiolate.

$K[O_2CC{\equiv}CH]$. Potassium propiolate is more hygroscopic than the sodium homologue. That H_2O smoothly enters and leaves the K^+ coordination sphere is apparent from the results shown in Figure 3. If a $MeOH/H_2O$ solution of the salt is evaporated on a BaF_2 plate, modes assignable to coordinated H_2O and partially displaced RCO_2^- appear. In the dry atmosphere of the spectrometer, the H_2O gradually escapes and the RCO_2^- returns to the coordination sphere after about 1 h, giving the spectrum of the anhydrous salt corresponding to that shown in Figure 1. With the readdition of $MeOH/H_2O$, the process shown in Figure 3 is repeatable. By DSC, the hydrated sample displays an endotherm corresponding to the loss of H_2O at about 60 °C and a double exotherm at 197 and 201 °C due to the decomposition of the salt. By TGA, the hydrated sample loses 1 equiv of H_2O at about 50 °C. This fact and the elemental analysis confirm that the hydrated sample is $K[O_2CC{\equiv}CH]{\cdot}H_2O$. Therefore, a scrupulously dried sample of this salt is needed to compare with the sodium salt.

Anhydrous $K[O_2CC{\equiv}CH]$ displays a small exotherm in the DSC at 180–185 °C followed by the large decomposition exotherm ($\Delta H = 920 \pm 150$ J/g) centered at about 195 °C. The onset of weight loss by TGA coincides with this second exotherm. The sample turns black when the atmosphere is N_2, but remains white if the decomposition is performed in air. Because of intumescence, the initial weight loss is difficult to quantify by TGA, but it is about 15–20% of the original sample weight. The IR spectrum of the residue revealed the major product to be K_2CO_3 along with a very small amount of $K_2C_2O_4$. Reaction 1 describes the thermal decomposition process.

Slow thermal decomposition of a thin film of anhydrous $K[O_2CC{\equiv}CH]$ supported between two BaF_2 plates forms a residue closely resembling that of the sodium salt (Figure 2), but differing from the products of reaction 1 obtained without confinement. The C≡C and CH modes disappear at about 191 °C and are replaced by modes representing another RCO_2^- species. No C=C or new CH modes are present in this dark brown residue. A true poly(propiolate) is probably not formed by this thermal treatment because the characteristic C=O and C=C modes at 1700 and

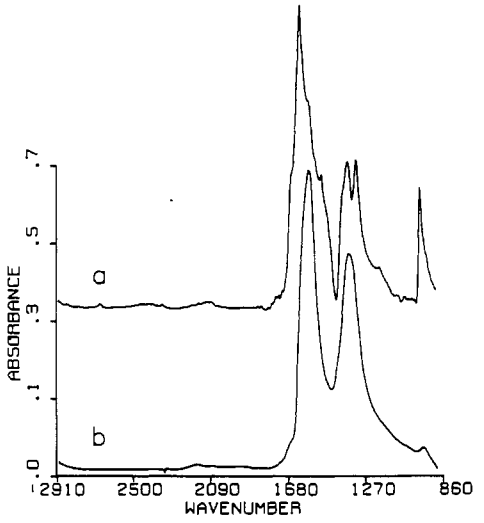

Figure 4. IR spectrum of an authentic sample of $K_2[O_2CC{\equiv}CCO_2]$ (a) compared to that of the residue from thermal decomposition of $K[O_2CC{\equiv}CH]$ between two BaF_2 plates (b).

1620 cm^{-1}, respectively, of poly(propiolic acid)[15] are not present. A much closer match exists between the residue spectrum and that of an authentic sample of potassium acetylenedicarboxylate, $K_2[O_2CC{\equiv}CCO_2]$, as shown in Figure 4. Although not a perfect correlation, it is the best yet found given the fact that the decomposition residue may not be a pure product. There is no resemblance of the residue to potassium fumarate or potassium maleate. Hereafter, the residue will be referred to as an acetylenedicarboxylate, although it is not firmly proven to be such. An acetylenedicarboxylate could be formed by reaction 2. This

$$4K[O_2CC{\equiv}CH] \xrightarrow{\Delta} 2K_2[O_2CC{\equiv}CCO_2] + 2C_2H_2 \quad (2)$$

reaction contrasts with (1) in that it involves a coupling process. The C≡C mode of the salt would not be detected by IR spectroscopy. This residue can be dissolved in H_2O and reprecipitated to yield the same IR spectrum. Fast thermolysis of the residue produced only CO and CO_2 with no evidence of C_2H_2 or H-containing products. All of these facts are consistent with a reaction resembling (2) occurring during the thermolysis of confined samples of the K^+ and Na^+ salts.

Thus, a fundamentally different thermolysis reaction occurs in the potassium and sodium propiolate salts depending on whether the thermal decomposition takes place in the confined state between two BaF_2 plates or in the unconfined state in a DSC or TGA pan. There is evidence of coupling reactions in the residue of the confined state, whereas metal carbonates form in the unconfined state. However, under certain circumstances, it is possible that the coupled product is not detected because it has thermally decomposed. We found experimentally that an authentic sample of $K_2[O_2CC{\equiv}CCO_2]$ decomposes, releasing CO_2 (no CO) about 200 °C. Hence, the decarboxylation reaction 3 summarizes the

$$4K[O_2CC{\equiv}CH] \xrightarrow{\Delta} 2K_2CO_3 + CO_2 + 2C_2H_2 + 5C \quad (3)$$

overall process because both (3) and the formation and decomposition of $K_2[O_2CC{\equiv}CCO_2]$ are net decarboxylation processes. A coupling reaction stopping at (2) would be favored when the chance for coupling is optimized (i.e., in the confined state), while reaction 3 becomes favored over reaction 1 as the lattice energy decreases. This is because reaction 3 is expected to be thermodynamically favored over reaction 1 and, thus, is favored by a lower decomposition temperature. In keeping with the trend in the decomposition temperature of $Na^+ > K^+$, reaction 3 will be shown in a moment to contribute more for K^+ than Na^+. This pattern continues in the data for the Rb^+ salt where reactions 2 and 3 completely dominate reaction 1.

(14) Schutte, C. J. H.; Buijs, K. *Spectrochim. Acta* **1964**, *20*, 187.

(15) Masuda, T.; Kawai, M.; Higashimura, T. *Polymer* **1982**, *23*, 744.

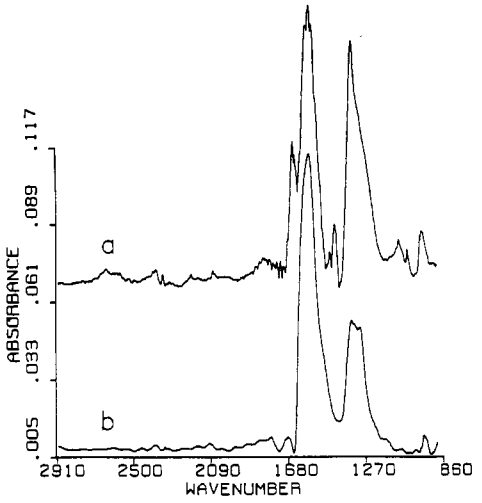

Figure 5. Comparison showing the similarity of the IR spectrum of the residue from $Rb[O_2CC{\equiv}CH]$ heated to 200 °C in a TGA pan (a) and that of the residue formed by thermolysis between two BaF_2 plates (b).

$Rb[O_2CC{\equiv}CH]\cdot 0.5[HO_2CC{\equiv}CH]$. Elemental analysis, DSC, TGA, and IR spectroscopy confirm that rubidium propiolate is solvated by propiolic acid. It is a hemisolvate in our hands. This causes the initial thermal behavior to differ from those of the Na^+ and K^+ salts. First, the process of acid evolution disrupts the crystal lattice to the point that a melting endotherm occurs at 125 °C by DSC. This endotherm immediately transits to an exotherm centered at 129 °C. At this temperature there is a weight loss in the TGA corresponding to 0.5 $HO_2CC{\equiv}CH$. The sample is visually observed to solidify after the endotherm, making it very probable that the exotherm results from crystallization of the sample. The IR spectrum of this newly crystallized product closely resembles those of the acid-free K^+ and Na^+ salts. Two exotherms at 162 °C (77 ± 30 J/g) and 169 °C (135 ± 50 J/g) then occur in the decomposition region of $Rb[O_2CC{\equiv}CH]$. These ΔH values are much smaller than those for the corresponding steps of the Na^+ and K^+ salts. No additional exotherms occur below 500 °C.

Visual examination of the sample at the two exotherms and of the remaining brown residue reveals much less intumescence than occurred for the Na^+ and K^+ salts. The IR spectrum of the residue also strongly differs from those of the Na^+ and K^+ salts in that only weak absorptions attributable to CO_3^{2-} and $C_2O_4^{2-}$ are present. Instead, the IR spectrum resembles that of the residue when the thermal decomposition is carried out between two BaF_2 plates (Figure 5). No C≡C, C=C, or CH modes are apparent. By reference to Figure 4, the product resembles an acetylenedicarboxylate, suggesting that the thermal decomposition of $Rb[O_2CC{\equiv}CH]$ is dominated by the coupling reaction 2. However, it is possible that a higher molecular weight product has formed because the weight loss at this step by TGA is only about 7% of the sample mass. The small amount of Rb_2CO_3 originates from reaction 3. Because less gas is produced during the coupling reaction, the intumescence is less and the sample is not blown from the TGA pan. If the heating is continued to 600 °C, the residue gradually loses weight and levels off at about the weight of Rb_2CO_3. The IR spectrum confirms the residue to be Rb_2CO_3.

Fast Thermal Decomposition of $M[O_2CC{\equiv}CH]$ ($M = Na^+, K^+, Rb^+$)

The fast thermal decomposition of the group IA propiolate salts was investigated by rapid-scan FTIR/temperature profiling.[9] This technique provides simultaneous, real-time, thermal measurements of the condensed phase and spectra of the near-surface gas products produced by rapid heating. An inert atmosphere was used so that the intrinsic thermolysis characteristics of the salt are learned rather than pathways disguised by the reactions with atmospheric O_2. The results corroborate and further support all of the findings of the slow thermolysis studies because the gas products from reactions 1–3 can be observed during the thermal events. In particular, the relative importance of the decarbonylation process (reaction 1) and the coupling and decarboxylation processes (reactions 2 and 3) can be assessed under a variety of conditions when rapid heating is applied under various Ar pressures. The assessment is made through the gas product ratios produced by each salt. Table I gives the data. Numerous studies were conducted at different heating rates and pressures. Only selected, representative results are described here.

Table I. Gas Product Ratios from the Fast Thermolysis of Propiolate Salts at Various Pressures and Heating Rates

		product ratio		
	psi of Ar	Na^+	K^+	Rb^+
CO/CO_2[a]	2	0.5 ± 0.1	0.2 ± 0.7	0
	15	0.8 ± 0.2	0.35 ± 0.07	0
	200	1.2 ± 0.2	0.45 ± 0.02	0
	500	1.5 ± 0.2	0.6 ± 0.15	0.1
C_2H_2/CO_x[b]	15	1.7 ± 0.2	2.7 ± 0.3	5

[a] dT/dt = 80–300 °C/s; ratios taken 1 s after the onset of decomposition. [b] x = 1, 2; dT/dt = 80–300 °C/s; ratios taken 1 s after the onset of decomposition.

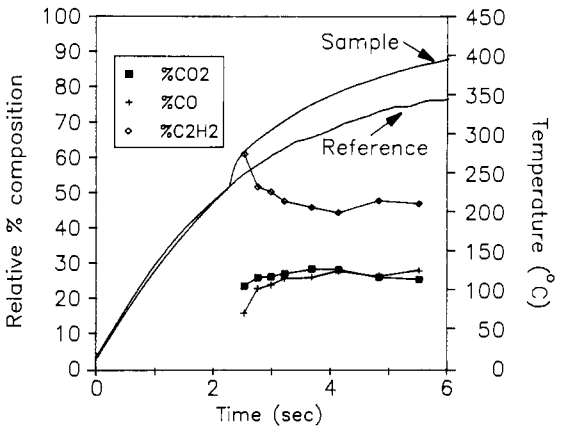

Figure 6. Relative percent composition of the gas products from the fast thermolysis of $Na[O_2CC{\equiv}CH]$ superimposed on the temperature profile of the condensed phase. The pressure was 200 psi of Ar.

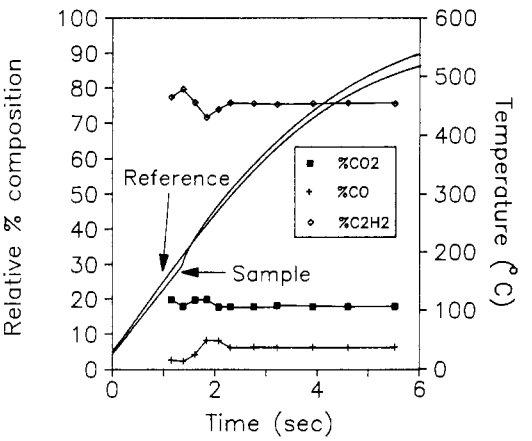

Figure 7. Relative percent composition of the gas products from the fast thermolysis of $K[O_2CC{\equiv}CH]$ superimposed on the temperature profile of the condensed phase. The pressure was 15 psi of Ar.

$Na[O_2CC{\equiv}CH]$ and $K[O_2CC{\equiv}CH]$. When 1 mg of dry $Na[O_2CC{\equiv}CH]$ is heated at an initial rate of 115 °C/s under 200 psi of Ar, a decomposition exotherm occurs at about 220 °C (Figure 6). This temperature compares to that of 203 °C obtained by DSC, but the agreement is reasonable based on the fact that the heating rate and pressure are so different. All of the gas decomposition products (CO, CO_2, C_2H_2) are detected simultaneously. The appearance of both CO and CO_2 indicates that partial decarbonylation (reaction 1) and partial decarboxylation (reaction 3) occur. Since there is no evidence that unconfined $Na[O_2CC{\equiv}CH]$ forms coupled products, it is probable that re-

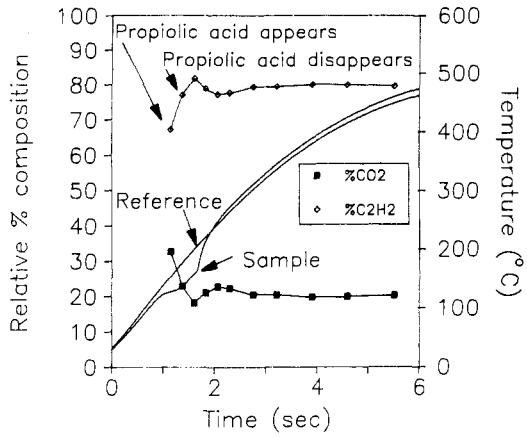

Figure 8. Relative percent composition of the gas products from fast thermolysis of $Rb[O_2CC{\equiv}CH]{\cdot}0.5[HO_2C{\equiv}CH]$ superimposed on the temperature profile of the condensed phase. The pressure was 15 psi of Ar.

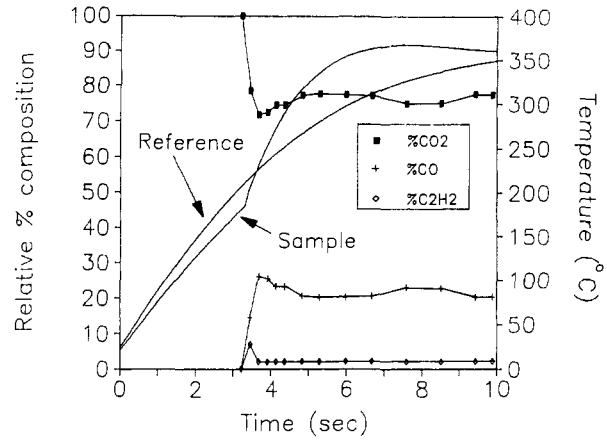

Figure 9. Relative percent composition of the gas products from fast thermolysis of $K[O_2CC{\equiv}CH]$ superimposed on the temperature profile of the condensed phase when the thermolysis was performed in air at atmospheric pressure.

action 2 is not involved. CO, CO_2, and C_2H_2 are the expected gases when Na_2CO_3 is the solid residue. Na_2CO_3 is confirmed to be the main solid product.

$K[O_2CC{\equiv}CH]$ reacts to fast thermolysis in essentially the same manner as the Na^+ salt except that the CO/CO_2 and C_2H_2/CO_x ratios are reproducibly different. Figure 7 shows a representative result. The exotherm occurs at about 190 °C compared to about 195 °C by DSC. As shown in Table I, more CO_2 than CO is generated indicating that the decarboxylation reaction 3 now dominates the decarbonylation reaction 1. This trend is consonant with the lower decomposition temperature of the K^+ salt compared to the Na^+ salt. Moreover, the observed larger C_2H_2/CO_x ratio is expected from the fact that the C_2H_2/CO_x ratio is twice as large for reaction 3 than for reaction 1.

$Rb[O_2CC{\equiv}CH]{\cdot}0.5[HO_2C{\equiv}CH]$. The trend established by the Na^+ and K^+ salts continues in the results for $Rb[O_2CC{\equiv}CH]{\cdot}0.5[HO_2CC{\equiv}CH]$ as shown in Figure 8. A pronounced melting endotherm occurs at about 125 °C. Propiolic acid absorptions appear in the gas phase at this point, but disappear rapidly probably because of condensation of the cool cell walls. No other salt studied releases propiolic acid upon thermolysis. An exotherm occurs at about 160 °C. Gases begin to be released shortly before this exotherm. Recall that a coupled product dominates in the residue of $Rb[O_2CC{\equiv}CH]$ along with some Rb_2CO_3 in this temperature range. In accordance with this, CO_2 is the only CO_x product detected because reaction 1 is shut down in favor of reactions 2 and 3. C_2H_2 is also released as required by reactions 2 and 3. Following the trend set by the Na^+ and K^+ salts, the decarboxylation and coupling processes increasingly dominate decarbonylation as the decomposition temperature of the salt decreases. Hence, the coupled product in the condensed phase, the low amount of intumescence and weight loss, the presence of CO_2 without CO in the gas phase, and the presence of a small amount of Rb_2CO_3 are all consistent and expected if thermolysis of $Rb[O_2CC{\equiv}CH]$ leads to coupling reactions represented by reaction 2. This behavior contrasts with the Na^+ and K^+ salts, where the decomposition temperature is higher and, thus, decarbonylation by reaction 1 is more important. We attribute this trend to the difference in lattice energy of the salts, $Na^+ > K^+ > Rb^+$ (vide infra).

When the thermolysis of all three salts is performed in air, CO and CO_2 vastly dominate because ample O_2 is available. The exotherm for the oxidation processes is large, but gradual. Figure 9 illustrates these points for $K[O_2CC{\equiv}CH]$. The thermolysis of these salts in air is apparently controlled by radical reactions with O_2. The gradual slope of the exotherm suggests that the decomposition resembles smoldering rather than ignition.

General Patterns for $M[O_2CC{\equiv}CH]$ ($M = Na^+, K^+, Rb^+$) Thermolysis

Slow thermolysis of the Na^+ and K^+ salts produces only intumescent carbonates, oxalates, and carbon, along with low molecular weight gases. However, with confinement of the sample, thermolysis induces coupling reactions. Coupling reactions occur in both the confined and unconfined state for the Rb^+ salt. The residue resembles a coupled carboxylate. Further details about the residue were not pursued beyond verifying these facts.

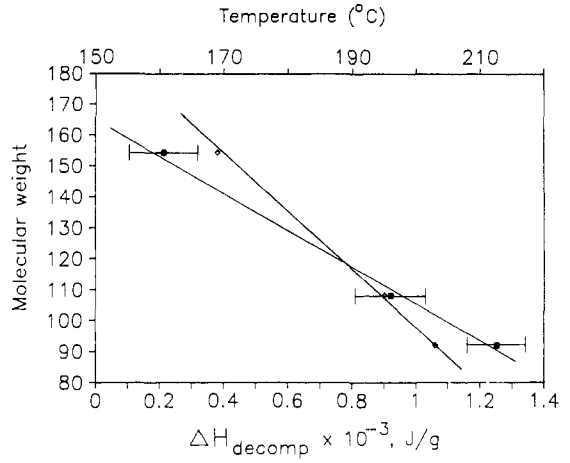

Figure 10. Correlation of the temperature (◇) and the total ΔH (■) for the exothermic decomposition steps of $M[O_2CC{\equiv}CH]$ ($M = Na^+, K^+, Rb^+$) with the molecular weight.

The reason for the different slow thermolysis patterns of these salts is suggested by Figure 10. Both the thermal decomposition temperature and the average ΔH for the main exothermic thermolysis steps are a function of the molecular weight of the salts at the decomposition point: the lower the molecular weight, the higher the values of ΔH and the temperature of decomposition. Thus, the difference in the energy released in the decomposition step is mainly caused by the dilution of ΔH (J/g) by the cation mass. The lattice energy changes in the same trend. With an increase in the atomic weight of the cation (decrease in the lattice energy), the decomposition process favors the lower energy pathways. Thus, the milder coupling reactions can occur in preference to total destruction of the organic component and liberation of low molecular weight gases. Davidov et al.[1] previously speculated that polymerization of propiolate salts induced by γ-radiation might increase with a decrease in the lattice energy. At least within this limited series, their speculation is confirmed by our findings. The lattice energy follows the trend $Rb^+ < K^+ < Na^+$. In accordance, we find that the tendency toward coupling is the reverse of this trend.

The gases liberated upon fast thermolysis are fully understandable with the above description. The importance of decarbonylation (CO, C_2H_2) relative to decarboxylation (CO_2, C_2H_2) and coupling shifts as expected on the basis of the decomposition temperatures of these salts. At the lower decomposition temperatures (Rb^+) only decarboxylation and coupling occur. At

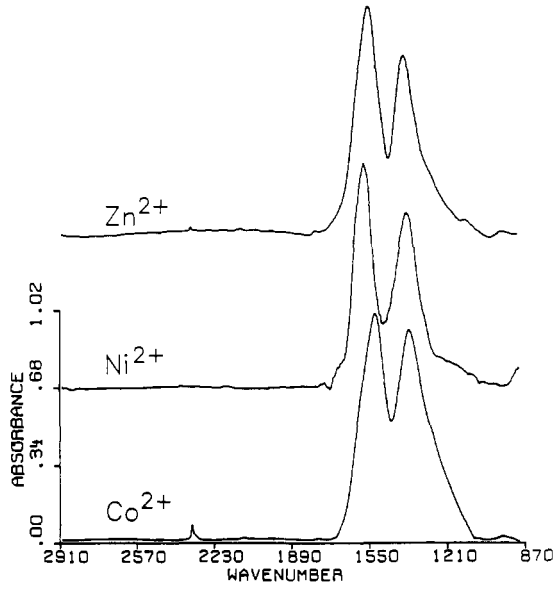

Figure 11. IR spectra of the residues from thermal decomposition of $Zn[O_2CC{\equiv}CH]_2{\cdot}2H_2O$, $Ni[O_2CC{\equiv}CH]_2$, and $Co[O_2CC{\equiv}CH]{\cdot}3H_2O$ between two BaF_2 plates at 210 °C.

higher temperatures (Na^+, K^+) both decarbonylation and decarboxylation compete. This pattern is manifested in the different CO/CO_2 ratios for these salts (Table I), irrespective of the applied Ar pressure (2–500 psi). Likewise, the C_2H_2/CO_x ratio depends on the decomposition temperature of the sample. With a higher decomposition temperature, CO and CO_2 are both liberated because reactions 1 and 3 occur. Thus, the ratio is smaller. At lower decomposition temperatures, only decarboxylation and coupling occur (reactions 2 and 3) so that less CO_x is formed and the C_2H_2/CO_x ratio is higher. Finally, as the pressure is raised, the gas products spend a longer time in the hot zone owing to their shorter mean free path.[16] This causes the sample to reach a somewhat higher temperature that favors the decarbonylation reaction and increases the CO/CO_2 ratio for all of the salts at higher pressures.

Thermolysis of Transition-Metal Propiolate Salts

The detailed studies above on Group IA propiolates make it possible to understand the general thermolysis patterns of more complicated metal propiolate salts, such as those of Co^{2+}, Ni^{2+}, and Zn^{2+}. In our hands, these salts have different amounts of water of hydration, which appear to mediate the thermolysis process. However, the general patterns are surprisingly consistent with the conclusions drawn about the anhydrous group IA salts and add confidence to the scenario developed above about the thermolysis process.

$Zn[O_2CC{\equiv}CH]_2{\cdot}2H_2O$. The first exotherm in the DSC (100 °C) appears to be associated with the loss of some H_2O. Accordingly, there is a weight loss in the TGA corresponding to about 0.5 H_2O, and H_2O is detected in the gas phase above the sample by IR spectroscopy. The appearance of gas decomposition products (CO_2, C_2H_2) in FTIR/temperature profiling at 160 °C approximates the temperature of weight loss (about 30% at 150 °C) in the TGA and the second exotherm in the DSC (ΔH = 340 J/g at 160 °C). The fact that CO_2 overwhelmingly dominates CO indicates that decarboxylation dominates the gas generation process. This is expected from the comparatively low thermal decomposition temperature. A reaction resembling (2) with some contribution from (3) is implicated because, as shown in Figure 11, the IR spectrum of the residue from the slow thermolysis between BaF_2 plates is very similar to the coupled products shown in Figure 2. The black residue from thermolysis of an unconfined sample also closely resembles that shown in Figure 11, indicating

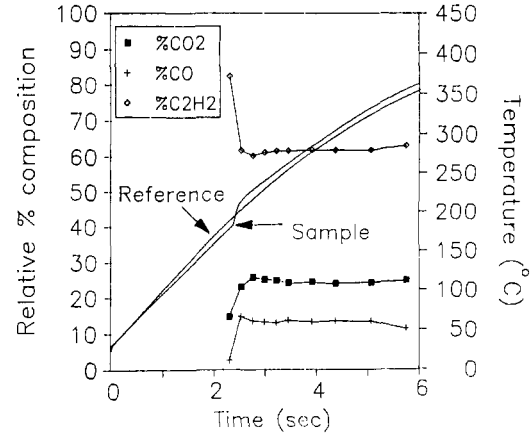

Figure 12. Relative percent composition of the gas products from the fast thermolysis of $Ni[O_2CC{\equiv}CH]_2$ superimposed on the temperature profile of the condensed phase. The pressure was 15 psi of Ar.

that coupling and decarboxylation describe the thermolysis process. This coupled product decomposes to $ZnCO_3$ if heated above 400 °C.

$Ni[O_2CC{\equiv}CH]_2$. This salt was investigated in the anhydrous form and, as such, behaves differently from the hydrated Zn^{2+} and Co^{2+} salts. It decomposes at a higher temperature in the DSC (ΔH = 920 J/g at 200 °C) than the hydrates. At this temperature there is a 30–40% weight loss, but intumescence makes it difficult to determine the exact percent. Owing to the high decomposition temperature, both decarbonylation and decarboxylation are expected. This is confirmed by the fact that both CO and CO_2 are evolved as shown in Figure 12. No coupling in the product residue is expected. Indeed, the IR spectrum of the black residue from thermolysis of an unconfined sample reveals only $NiCO_3$ with a small amount of NiC_2O_4. Hence, coupling reactions do not occur under these conditions. The Na^+ and K^+ salts, which also have higher decomposition temperatures, behave in the same way, but are different from the Zn^{2+}, Co^{2+}, and Rb^+ salts, which have lower decomposition temperatures. The residue produced by confined thermolysis between two BaF_2 plates (Figure 11) causes coupling as it does for all of the other salts.

$Co[O_2CC{\equiv}CH]_2{\cdot}3H_2O$. Purple $Co[O_2CC{\equiv}CH]_2{\cdot}3H_2O$ was the most difficult of the salts to characterize. Red $Co[O_2CC{\equiv}CH]_2{\cdot}4H_2O$ has been reported to decompose explosively.[4] The closely related purple salt studied here intumates the most vigorously of all compounds studied. This causes the sample to blow off the thermolysis filament or out of the TGA pan to the point that both the black decomposition solid and the parent material are always present in the residue. The sharp decomposition exotherm located at 161 °C in the well-dried purple trihydrate and 175 °C (875 J/g) in the red tetrahydrate indicates that, on the basis of the rather low temperature, decarboxylation and coupling reactions should dominate. Indeed, CO/CO_2 is less than 0.25, reflecting the emphasis toward decarboxylation. The IR spectra of the residues from the confined and unconfined thermolysis reactions are similar as shown in Figure 11. A coupled product is indicated. Thus, reaction 2 best describes the thermolysis process of this salt. However, the appearance of a weak absorbance at 2333 cm^{-1} suggests the presence of some $-C{\equiv}C-C{\equiv}C-$ linkages in the residue.

It was noted above that both ΔH_{dec} and the temperature of decomposition are qualitative indicators of the tendency of these salts to branch to a carbonate or to a coupled product upon thermolysis. ΔH_{dec} for these transition metal salts appears to be a less reliable indicator of the tendency to polymerize than the temperature of decomposition.

A possible reason was sought for the suggested explosive behavior of cobalt propiolates. By DSC, ΔH_{dec} is lower than that for the nonexplosive Na^+ salt so that the amount of heat released is not the reason. Instead, it seems probable that the rate of the gas release is more important because the DSC exotherm is sharp and the sample intumates so vigorously. Since the Co^{2+} salt has

(16) Oyumi, Y.; Brill, T. B. *Combust. Flame* **1987**, *68*, 209.

readily accessed alternate oxidation states, perhaps the ease of electron transfer in the radical steps is responsible for the apparent rate difference.

In summary, a detailed study of the thermolysis of group IA propiolate salts permits the thermolysis behavior of more complex transition-metal propiolates to be predicted and rationalized. The approximate gas product ratios and the tendency to form coupled products or carbonates can be judged from the decomposition temperatures alone of the salts.

Acknowledgment. We are grateful to Professor Bruce M. Foxman of Brandeis University for supplying several samples of propiolate salts and calling our attention to their interesting behavior. We are grateful to Morton-Thiokol, Inc., for financial support, and, especially, to Dr. David A. Flanigan for his willingness to let us continue the study of metal complexes.

Contribution from the Dipartimento di Chimica,
Università di Perugia, 06100 Perugia, Italy

UV Photochemistry of *trans*-Cyanothiocyanatotetraamminechromium(III). Communication between Charge-Transfer and Ligand-Field States

Pietro Riccieri, Edoardo Zinato,* and Antonella Damiani

Received August 3, 1988

Irradiation (at 295 and 250 nm) of the charge-transfer (CT) bands of *trans*-$Cr(NH_3)_4(CN)(NCS)^+$ in 1×10^{-3} M $HClO_4$/0.10 M $NaClO_4$ solution results in aquation of all three types of ligands. With respect to ligand-field (LF) photolysis, Φ_{NH_3} and Φ_{CN^-} decrease by 20%, while Φ_{NCS^-} increases up to 5-fold. The photoreactions are partially quenched by $Cr(C_2O_4)_3^{3-}$, which also completely quenches the LF doublet-state emission. The limiting unquenchable quantum yields differ from the LF ones, and from comparison of the two quenching patterns, the efficiency for CT → LF internal conversion is determined to be $\eta_{IC} = 0.6$. This is confirmed by the wavelength dependence of the relative phosphorescence quantum yields. Also, the intrinsic CT photoreactivity is evaluated ($\Phi^\circ_{CT} = 0.05$–0.09). The predominance of NCS^- loss is consistent with the NCS-to-Cr CT transition, and primary photoredox activity is demonstrated by Cr(II) scavenging.

The charge-transfer (CT) photochemistry of chromium(III) complexes has not received as much attention as the ligand-field (LF) photochemistry. This is not surprising, since LF excited states, hence photosubstitution reactions,[1-3] have been the focus of all photolysis models.[3-9] That CT states of chromium(III) have their own chemistry is indicated by a number of changes observed on passing from LF to CT excitation. The quantum yields for aquation of one or more ligands often increase considerably.[10-14] New reaction modes may take place.[15-21] Redox products are sometimes revealed by flash photolysis[17,18,21-27] or Cr(II) scavenging.[16,17,24,28] However, little quantitative information is available on such chemistry, as it is generally superimposed on LF reactivity, consequent to CT → LF internal conversion. Because of the high reducing power of Cr(II), the primary CT redox products either partially or totally end up as substitutional species, often indistinguishable from those originated in the lower lying LF states. Related to this problem is the lack of knowledge on the efficiency of communication between the CT and LF manifolds.

Some chromium(III) systems do exhibit peculiar LF properties, as doublet-state emission and quenchability of photosubstitutions, which may be taken advantage of to unambiguously separate the CT from the LF photobehavior. Several features make the *trans*-$Cr(NH_3)_4(CN)(NCS)^+$ ion suitable for this kind of approach. (i) Easy access to CT states is provided by a band-rich UV spectrum, spread over a wide wavelength range. (ii) The well-characterized LF photochemistry consists of three simultaneous and comparably efficient reactions.[29] (iii) Reasonably intense and long-lived phosphorescence is emitted under photolysis conditions.[29]

Experimental Section

The *trans*-$[Cr(NH_3)_4(CN)(NCS)](ClO_4)$ salt was synthesized as already reported.[29] Besides the LF maxima at 466 (ϵ 80.0 M^{-1} cm^{-1}) and 355 nm (ϵ 51, shoulder), the absorption spectrum in aqueous medium exhibits intense CT bands at 298 (ϵ 3700), 252 (ϵ 2800, sh), 228 (ϵ 8400), and 210 nm (ϵ 6700, shoulder), as illustrated in Figure 1. $K_3[Cr(C_2-$

(1) Zinato, E. In *Concepts of Inorganic Photochemistry*; Adamson, A. W., Fleischauer, P. D., Eds.; Wiley: New York, 1975; Chapter 4.
(2) Kirk, A. D. *Coord. Chem. Rev.* **1981**, *39*, 225.
(3) Endicott, J. F.; Ramasami, T.; Tamilarasam, R.; Lessard, R. B.; Ryu, C. K. *Coord. Chem. Rev.* **1987**, *77*, 1.
(4) Adamson, A. W. *J. Phys. Chem.* **1967**, *71*, 798.
(5) Pyke, S. C.; Linck, R. G. *J. Am. Chem. Soc.* **1971**, *93*, 5281.
(6) Zink, J. I. *J. Am. Chem. Soc.* **1972**, *94*, 8039; *Mol. Photochem.* **1973**, *5*, 151; *Inorg. Chem.* **1973**, *12*, 1957; *J. Am. Chem. Soc.* **1974**, *96*, 4464.
(7) Wrighton, M.; Gray, H. B.; Hammond, G. S. *Mol. Photochem.* **1973**, *5*, 165.
(8) Vanquickenborne, L. G.; Ceulemans, A. *J. Am. Chem. Soc.* **1977**, *99*, 2208; *J. Am. Chem. Soc.* **1978**, *100*, 475; *Inorg. Chem.* **1979**, *18*, 897; *Inorg. Chem.* **1979**, *18*, 3475.
(9) Vanquickenborne, L. G.; Ceulemans, A. *Coord. Chem. Rev.* **1983**, *48*, 157.
(10) Wasgestian, F.; Schläfer, H. L. *Z. Phys. Chem. (Munich)* **1968**, *62*, 127.
(11) Riccieri, P.; Schläfer, H. L. *Inorg. Chem.* **1970**, *9*, 727.
(12) Riccieri, P.; Zinato, E. *J. Am. Chem. Soc.* **1975**, *97*, 6071.
(13) Riccieri, P.; Zinato, E.; Sheridan, P. S. *Inorg. Chem.* **1979**, *18*, 720.
(14) Riccieri, P.; Zinato, E. *Inorg. Chim. Acta* **1981**, *52*, 133.
(15) Malati, M. A.; Rophael, M. W. *J. Inorg. Nucl. Chem.* **1966**, *28*, 915.
(16) Vogler, A. *J. Am. Chem. Soc.* **1971**, *93*, 5912.
(17) Sriram, R.; Endicott, J. F. *Inorg. Chem.* **1977**, *16*, 2766.
(18) Katz, M.; Gafney, H. D. *Inorg. Chem.* **1978**, *17*, 93.
(19) Yang, D. B.; Kutal, C. *J. Chem. Soc., Chem. Commun.* **1978**, 363.
(20) Ruminski, R. R.; Coleman, W. F. *Inorg. Chem.* **1980**, *19*, 2185.
(21) Marchaj, A.; Stasicka, Z.; Rehorek, D. *Polyhedron* **1983**, *2*, 1281.
(22) Fleischauer, P. D. Ph.D. Dissertation, University of Southern California, Los Angeles, 1968.
(23) Ohno, T.; Kato, S. *Bull. Chem. Soc. Jpn.* **1973**, *46*, 1602.
(24) Sriram, R.; Endicott, J. F. *J. Chem. Soc., Chem. Commun.* **1976**, 683.
(25) Ferraudi, G.; Yang, D. B.; Kutal, C. *J. Chem. Soc., Chem. Commun.* **1979**, 1050.
(26) Ferraudi, G.; Endicott, J. F. *Inorg. Chim. Acta* **1979**, *37*, 219.
(27) Kutal, C.; Yang, D. B.; Ferraudi, G. *Inorg. Chem.* **1980**, *19*, 2907.
(28) Sandrini, D.; Gandolfi, M. T.; Moggi, L.; Balzani, V. *J. Am. Chem. Soc.* **1978**, *100*, 1463.
(29) Riccieri, P.; Zinato, E.; Damiani, A. *Inorg. Chem.* **1987**, *26*, 2667.

0020-1669/89/1328-4506$01.50/0